J. Condensed Matter Nucl. Sci. 38 (2024) 245–268

Research Article

Possibility of Coherent LENR Dynamics with Nuclear Molecules

Peter L. Hagelstein

Massachusetts Institute of Technology, Cambridge, MA, USA

Abstract

Excess heat in the Fleischmann-Pons experiment is generated without commensurate energetic nuclear particle emission, which has often been used to argue that the effect is not nuclear. Instead, we have argued that a better interpretation is that excess heat is not a result of quantum mechanically incoherent processes. For many years we have pursued quantum mechanically coherent models in which excess heat production is a byproduct of an underlying coherent nuclear process, of which fusion is a part of. A major difficulty with this approach has always been an inability to identify reasonably stable excited nuclear states that might support the required coherent nuclear dynamics, since only a modest number of metastable nuclei are known among all the stable isotopes. Here is proposed that nuclear molecules may provide a set of reasonably stable nuclear excited states. We use a simple cluster model based on the finite range liquid drop model to estimate excited state energies for nuclear molecules from the stable Pd isotopes. The highest density of states occurs near 50 MeV. A model is proposed in which generalized excitation transfer moves population to the high density of state region where efficient energy exchange with the lattice can occur. Excess heat is proposed to occur through a cycle in which excitation is promoted, where energy exchange occurs, followed by a multi-step return to the ground state. If this process is frustrated, then tunneling decay of highly-excited nuclear molecules results in transmutation.

Keywords: Fleischmann-Pons excess heat, coherent nuclear dynamics, theory, nuclear molecules, evolution equations

1. Introduction

We have long focused on the possibility that the anomalies in LENR are due to coherent dynamics among nuclear states driven by coupling with low energy collective degrees of freedom of the metal hydride or deuteride. A headache that has plagued this approach since the beginning is that highly-excited nuclei must be involved for any such scheme to work, but highly excited nuclei tend to be short-lived, which is problematic for coherent nuclear dynamics.

In a brainstorm in April of 2022 emerged the possibility that nuclear molecules might be involved in connection with excess heat and transmutation. An earlier naive version of the idea can be found in [1] in connection with speculations concerning lattice-induced fission in the Cardone experiments and Carpinteri experiments. Following a frantic few months of work a preliminary account of the approach was presented at ICCF24. Since then there has been some clarification of the approach, and a brief account will be given in what follows.

The notion of a nuclear molecule was introduced in response to the observation of resonances in collisions between ^{12}C nuclei [2], [3]. Two nuclei close together at the fermi scale have the possibility of forming a nuclear molecule, by analogy at the atomic scale of molecules formed through electron bonding [4]. Earlier work on nuclear fission proposed essentially the same notion [5]. By now the notion of nuclear molecules is accepted within nuclear physics.

Bohr and Wheeler suggested the use of the liquid drop model to describe this kind of nuclear structure [5]. The basic idea in this kind of model is that the nucleus is modeled as a droplet with constant mass and charge density, with a constant (attractive) nuclear energy linear in the volume, a (repulsive) energy proportional to the surface area, and a (repulsive) Coulomb energy connected with the electric charge density. In a liquid drop model of a nuclear molecule, the volume energy is the same as in a spherical version of the nucleus, but the Coulomb energy can be decreased by the separation of charge, and the surface energy is increased due to the larger surface associated with the nuclear molecule. In this kind of model, the spherical configuration has minimum energy, but nuclear molecule states have a local minimum in energy at high excitation energies.

A significant advantage of this kind of model is that it can predict ground state energies of nuclei over a wide range of mass and charge with reasonably good accuracy [6], [7]. More sophisticated versions of the model have been developed over the years for modeling deformation associated with fission and fusion (see [8], [9], [10]).

Most nuclear molecule calculations in the literature are focused on (1) fission of heavy nuclei; (2) resonances in (heavy) nuclear collisions; and (3) resonances symmetric light systems such and C-C and O-O. Binary nuclear molecules were the focus of early research, but subsequently calculations have been published with results for ternary nuclear molecules and more complicated structures as well. At present there are no systematic studies available that provide an assessment of nuclear molecule states in Pd nuclei that might be of interest in LENR.

We draw attention to a subtle issue that will be important in the discussion to follow. Nuclear molecules with low rotational angular momentum near Pd predicted for a fission or fusion model are not expected to be stable against tunnel decay. A “nuclear molecule” made of two daughters modeled as “clusters” that nearly touch are expected in general to be much more stable against tunnel decay. In the literature such states tend to be referred to in connection with clusters, as distinct from nuclear molecules. In this paper we will use a nuclear molecule terminology in connection with both kinds of models.

A number of issues are of interest. For example, are nuclear molecule (cluster) states predicted? If so, at what energies? How stable are they? And can they be accessed through interactions with condensed matter degrees of freedom? We have recently explored models for nuclear molecules, which allows us to begin addressing some of these questions.

In Sections 2 and 3 we consider the two different models for nuclear molecules from the Pd isotopes. An important conclusion is that there reasonably stable binary nuclear molecules are not expected from liquid drop models as normally used for fission calculations. Calculations done for C-C and for O-O suggest that there should be reasonably stable nuclear molecule states which involve clusters rather than extreme nuclear deformation. We consider the possibility that reasonably stable nuclear molecules can be modeled systematically based on this picture, and we propose a simplified model for the nuclear molecule energies and tunneling decay rates. In the following sections we consider the issues involved, what kind of scheme might be involved, and what a model might look like. The conclusion is that this approach results in a model which has the potential to be closely connected to experiment. Unfortunately, the resulting model is complicated, and accurate energy levels and transition matrix elements are not available.

In Section 4 we consider issues associated with coherent energy exchange, and their impact on schemes to model excess heat production. In Section 5 we consider a candidate scheme for excess energy production in PdD_x. In Section 6 we begin thinking about modeling the associated coherent dynamics. Conclusions appear in Section 7.

2. Bohr-Wheeler Approach

The focus in the first part of this study is on a basic liquid drop model, seeking optimized surfaces and excitation energies for symmetric and asymmetric binary nuclear molecules. The idea is that since we have not worked with these models previously, that there would be much to learn by working with the simplest relevant model. Even though the model is simple, the numerical optimization of the surface is not straightforward.

Nuclear molecules can rotate, which is important for ion-ion collisions. However, rotating nuclear molecules undergo radiative decay, which reduces their lifetime, making them perhaps less suitable for the coherent dynamics of interest in what follows. Hence, the focus here will be on non-rotating nuclear molecules.

2.1. Basic Liquid Drop Model

We worked with a Bohr-Wheeler liquid drop model based on

$$E \;=\; -B_V' \int_V d^3\mathbf{r} + B_S \oint_S d^2a + \frac{1}{2}\frac{Z(Z-1)}{Z^2}\int\int \frac{\rho_C(\mathbf{r})\rho_C(\mathbf{s})}{4\pi\epsilon_0|\mathbf{r}-\mathbf{s}|}d^3\mathbf{r}d^3\mathbf{s} \tag{1}$$

The first term on the RHS accounts for the volume and antisymmetry energy, the second accounts for the surface energy, and the third term is the Coulomb energy where $\rho_C(\mathbf{r})$ is the charge density assumed constant within the deformed nucleus. We scaled the Coulomb energy by the factor $Z(Z-1)/Z^2$ as appropriate for a nucleus made of Z discrete protons. We used values for the fitting parameters given by

$$\begin{aligned} B_V &= 1.946 \text{ MeV/fm}^3 \\ B_S &= 0.834 \text{ MeV/fm}^2 \\ B_A &= 0.047 \text{ MeV/fm}^3 \\ B_V' &= B_V - B_A \;=\; 1.899 \text{ MeV/fm}^3 \end{aligned} \tag{2}$$

These correspond to the more conventional liquid drop fitting parameters

$$\begin{aligned} a_V &= 14.8 \text{ MeV} \\ a_S &= 15.6 \text{ MeV} \\ a_A &= 20.3 \text{ MeV} \end{aligned} \tag{3}$$

corresponding to the more conventional liquid drop parameterization

$$E \;=\; a_V A + a_S A^{2/3} + a_C\frac{Z(Z-1)}{A^{1/3}} - a_A\frac{(N-Z)^2}{A} + \delta(N,Z) \tag{4}$$

The total energy in the spherical liquid drop model is made up of the volume energy, surface energy, Coulomb energy, symmetry (or Pauli) term and pairing term. For this model we have taken the spherical liquid drop radius to be

$$R \;=\; 1.22\, A^{1/3} \text{ fm} \tag{5}$$

The liquid drop model volume, surface and asymmetry terms were developed from least squares optimization of mass energies in the mass range near $A = 100$.

In the calculation of deformed surfaces using the liquid drop model, the nuclear volume is taken to be an invariant. Hence, the optimization in this version of the model depends on the Coulomb and surface terms, and not on the volume energy (which can be absorbed into the Lagrange multipliers in the optimization). When we optimized values of the liquid drop model parameters, the mean square error and fitting parameter for the surface energy depended only weakly on whether the pairing term was included or not. So the fitting parameters given were optimized without including the pairing energy.

2.2. Surface Parameterization

We initially developed a code to optimize a general surface characterized by cylindrical ρ_j values corresponding to z_j points. This was not straightforward as the associated Jacobian matrix for the corresponding Newton iterations is unstable, and there are headaches associated with the boundary conditions. Nevertheless, we were able to get convergence resulting in optimum solutions for a number of test problems.

From this experience we were motivated to try an approach that was closer to what is discussed in the literature. We used a parameterization given by

$$\rho(z) \;=\; \sqrt{\sum_j \rho_j^2 L_j(z)} \tag{6}$$

which involves approximating the square of the radial values in cylindrical coordinates with Lagrange interpolants. A simple version of the model was developed based on uniform spacing of points in z, from one boundary of the nuclear molecule to the other. We worked with up to 15 points, which includes two boundary points with zero fitting parameters.

2.3. Optimization

Optimization was based on the variational quantity I

$$I \;=\; E_C - B'_V V + B_S S - \lambda_b V_b - \lambda_c V_c \tag{7}$$

The optimum surface (characterized by a vector $\mathbf{c}_0$ made up of the fitting coefficients $c_j = \rho_j^2$) satisfies

$$(\nabla I)_{\mathbf{c}_0} \;=\; \mathbf{0} \tag{8}$$

or

$$(\nabla E_C)_{\mathbf{c}_0} - B'_V(\nabla V)_{\mathbf{c}_0} + B_S(\nabla S)_{\mathbf{c}_0} - \lambda_b(\nabla V_b)_{\mathbf{c}_0} - \lambda_c(\nabla V_c)_{\mathbf{c}_0} \;=\; \mathbf{0} \tag{9}$$

Around the optimum we can write

$$(\nabla I)_{\mathbf{c}} \;=\; (\nabla I)_{\mathbf{c}_0} + \mathbf{K}_I \cdot (\mathbf{c} - \mathbf{c}_0) \;=\; \mathbf{K}_I \cdot (\mathbf{c} - \mathbf{c}_0) \tag{10}$$

where $\mathbf{K}_I$ is the Jacobian of I with respect to the c_j. The formal solution for the Newton's iteration correction is then

$$(\mathbf{c}_0 - \mathbf{c}) \;=\; -\,\mathbf{K}_I^{-1} \cdot (\nabla I)_{\mathbf{c}} \tag{11}$$

We can expand this to read

$$(\mathbf{c}_0 - \mathbf{c}) \;=\; -\,\mathbf{K}_I^{-1} \cdot \left\{ (\nabla E_C)_{\mathbf{c}} - B'_V(\nabla V)_{\mathbf{c}} + B_S(\nabla S)_{\mathbf{c}} - \lambda_b(\nabla V_b)_{\mathbf{c}} - \lambda_c(\nabla V_c)_{\mathbf{c}} \right\} \tag{12}$$

We used an inequivalent Jacobian based on

$$\mathbf{K}_I \;\approx\; \mathbf{K}_C + B_S \mathbf{K}_S \tag{13}$$

where the Jacobians of the individual volumes are neglected (the Jacobian of the total volume vanishes). We define vectors according to

$$\mathbf{x}_C \;=\; \mathbf{K}_I^{-1}(\nabla E_C)$$

$$\mathbf{x}_S \;=\; \mathbf{K}_I^{-1}(\nabla S)$$

$$\begin{aligned}\mathbf{x}_V &= \mathbf{K}_I^{-1}(\nabla V)\\ \mathbf{x}_{V_b} &= \mathbf{K}_I^{-1}(\nabla V_b)\\ \mathbf{x}_{V_c} &= \mathbf{K}_I^{-1}(\nabla V_c)\end{aligned} \tag{14}$$

It follows that the correction is

$$(\mathbf{c}_0 - \mathbf{c}) \ = \ -\mathbf{x}_C + B_V'\mathbf{x}_V - B_S\mathbf{x}_S + \lambda_b\mathbf{x}_{V_b} + \lambda_c\mathbf{x}_{V_c} \tag{15}$$

The volumes associated with the two daughters is specified initially, and remains (approximately) constant during the iterations. For this we require that

$$\begin{aligned}(\nabla V_b)_{\mathbf{c}}\cdot(\mathbf{c}-\mathbf{c}_0) &= 0\\ (\nabla V_c)_{\mathbf{c}}\cdot(\mathbf{c}-\mathbf{c}_0) &= 0\end{aligned} \tag{16}$$

where $(\nabla V_b)_{\mathbf{c}}$ and $(\nabla V_c)_{\mathbf{c}}$ are the gradients of the daughter volumes with respect to the fitting parameters. These can be written as

$$\begin{aligned}(\nabla V_b)\cdot\Big\{-\mathbf{x}_C + B_V'\mathbf{x}_V - B_S\mathbf{x}_S + \lambda_b\mathbf{x}_{V_b} + \lambda_c\mathbf{x}_{V_c}\Big\} &= 0\\ (\nabla V_c)\cdot\Big\{-\mathbf{x}_C + B_V'\mathbf{x}_V - B_S\mathbf{x}_S + \lambda_b\mathbf{x}_{V_b} + \lambda_c\mathbf{x}_{V_c}\Big\} &= 0\end{aligned} \tag{17}$$

This is equivalent to the linear equations

$$\begin{aligned}\Big((\nabla V_b)\cdot\mathbf{x}_{V_b}\Big)\lambda_b + \Big((\nabla V_b)\cdot\mathbf{x}_{V_c}\Big)\lambda_c &= (\nabla V_b)\cdot\mathbf{x}_C - B_V'(\nabla V_b)\cdot\mathbf{x}_V + B_S(\nabla V_b)\cdot\mathbf{x}_S\\ \Big((\nabla V_c)\cdot\mathbf{x}_{V_b}\Big)\lambda_b + \Big((\nabla V_c)\cdot\mathbf{x}_{V_c}\Big)\lambda_c &= (\nabla V_c)\cdot\mathbf{x}_C - B_V'(\nabla V_c)\cdot\mathbf{x}_V + B_S(\nabla V_c)\cdot\mathbf{x}_S\end{aligned} \tag{18}$$

2.4. Results and Discussion

We optimized the surface in terms of the Lagrange fitting parameters, as well as the overall distance from one end to the other of the deformed nucleus. With this parametrization, we found weakly bound nuclear molecule surfaces such as shown in Figure 1 for the symmetric case, which is reasonably close to the symmetric shape near $A = 100$ shown in [9]. In Figure 2 a surface is illustrated for the asymmetric case.

The barrier energy for the symmetric case (without correcting for the fission energy, which is different in this kind of model than experiment due in part to the fact that the Coulomb energy in the liquid drop model fit is less that the Coulomb energy calculated with in the model) is near 44 MeV, which is less than 10% higher than values in the literature from more sophisticated models.

The optimizations which we carried out led systematically to a local minimum of the energy with respect to the separation of the daughters, indicative of nuclear molecule formation. It is possible that this may be an artifact of the approach, due to the fact that there are multiple solutions for the surface at a given separation. The energy minima that we found involved optimizations in which the solutions are close over the energy range considered, and we did not optimize over all possible bands of solutions permitted by the model. Even if the solutions were taken as corresponding to physical states, the potential associated with the local potential minimum is sufficiently shallow that the daughters would tunnel apart in well under 10^{-20} seconds. These solutions are unfortunately not useful for coherent nuclear dynamics modeling of the kind we are interested in.

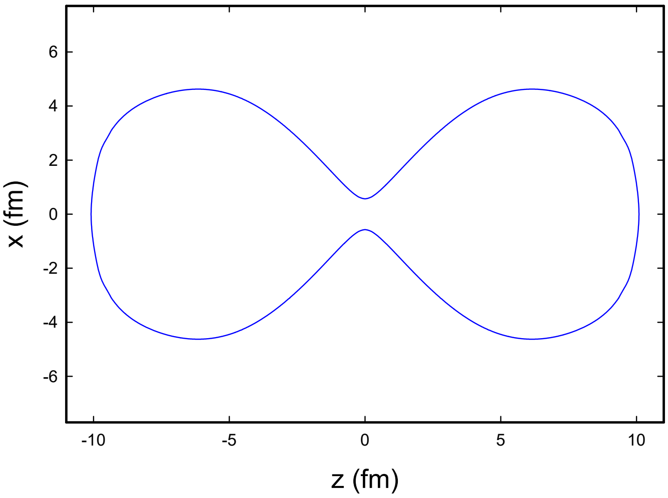

Figure 1. Liquid drop model surface for a symmetric binary nuclear molecule, where the parent $A = 106$ nucleus is split into two daughter nuclei with $A_b = A_c = 53$.

3. Finite Range Liquid Drop Model and Cluster Picture

Perhaps the most significant drawback of the Bohr-Wheeler model for describing fission and fusion processes is that the strong force interaction comes in through volume and surface energy terms, so that there is no residual strong force interaction when the daughters are separated.

A more sophisticated model that remedies this is the folded Yukawa model, such as discussed in [11]. In this model the strong force interaction is modeled through a scalar Yukawa potential between different elements of the liquid drop mass density, which leads to a short range daughter-daughter attraction as might be expected intuitively. One issue with this model is that it includes both volume and surface contributions for the strong force energy, which makes a connection with the LDM surface fit problematic. More important is that the spatial range of the Yukawa potential would be expected to be determined by the pion mass, but when compared with experiment this overestimates the range of the interactions for daughter-daughter interactions.

3.1. Finite Range Liquid Drop Model

Both of these issues are addressed in the finite range liquid drop model (FRLDM). It is possible to isolate approximately the surface contribution to the energy by subtracting an empirical exponential potential (the combination is referred to as the Yukawa plus exponential interaction, or YPE interaction), such that the contribution of the two terms to the volume energy vanishes. In this picture the Yukawa potential contribution to the volume energy is taken to be local, which greatly simplifies things. Once the surface contribution was isolated in this way, it was found that improved agreement with experiment could be obtained by allowing the range of the interaction to be a free parameter and optimizing. This resulted in a folded surface interaction with a shorter range than might have been expected based on the pion mass. The strength of the YPE interaction can be determined by matching to the surface energy of a liquid drop model optimization over the isotopic masses. This model is used with an additional charge density correction to

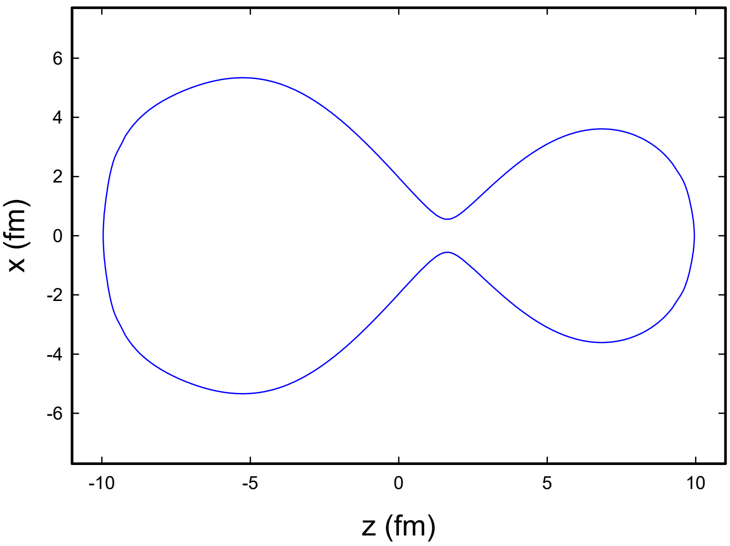

Figure 2. Liquid drop model surface for an asymmetric binary nuclear molecule, where the parent $A = 106$ nucleus is split into two daughter nuclei with $A_b = 80,\ A_c = 26$.

the Coulomb interaction, which contributes a minor correction to the shape and barrier energy. Relevant descriptions of the model are given in [8], [9].

Implementing the model into a code is greatly helped by equating the double volume integral of the folded YPE to an equivalent double surface integral (by making use of the Gauss-Ostrogradsky divergence theorem) as described in these references, and also in [12]. In our implementation we have made use of two-dimensional cubature formula in addition to Gaussian quadrature for the angular integration to evaluate efficiently the three-dimensional integrals that result. We used (older) model fitting parameters from [13].

This model was used for calculations of nuclear molecules along relevant to fission and fusion models similar to those calculated in the Bohr-Wheeler model described above. We found this more sophisticated model to be less stable than the Bohr-Wheeler model outlined above, so that useful results were not obtained with the Lagrange type of parametrization described above. We implemented a three region quadratic surface parametrization [14], along with quartic and sixth-order generalizations. Multiple branches of solutions were obtained with these models, which was a headache. The barrier energy for Pd-106 in our calculations was 40.7 MeV, in good agreement with the literature values. However, similar to the results obtained with the Bohr-Wheeler model, we did not find reasonably stable nuclear molecule solutions in connection with the fission barrier calculations.

3.2. Cluster Picture

We developed models for ^{12}C+^{12}C [15], [16], [17] and for ^{16}O+^{16}O [18], [19]. Comparisons with FRLDM nuclear molecule models appropriate for fission and fusion calculations led to the conclusion that there was no agreement with potentials from the literature. We tried instead working with models based on separated daughter nuclei, where we were able to get reasonable agreement with the potential shape and minimum.

After some consideration, this seems to be an important observation in connection with the development of a model for reasonably stable nuclear molecules. From the literature on fission models, and from a fission type of calculation with the FRLDM, one might not expect there to be a reasonably stable nuclear molecule state in these systems. Yet in the reference cited in this subsection (and in other papers as well) potential models are given which would predict a reasonably stable nonrotational nuclear molecule state. So, the question is, what is the difference in the associated physical pictures?

The conjecture here is that in these potential models, the carbon and oxygen daughter nuclei are essentially clusters which largely remain intact, and which attract one another when separated from each other but close within a few fm. The potential increases once the two nuclei begin to touch, which we might attribute to occupation of more highly excited states as the nucleons in the daughters rearrange to accommodate the deformation associated with moving into one another. In a fusion calculation at higher energy, the incoming nuclei have sufficient energy to overcome this initial barrier, and merge together as described approximately by a liquid drop model (appropriate for fission and fusion).

This suggests that there should be (at least) two basic regimes associated with nuclear molecule formation. In the higher relative kinetic energy regime, colliding nuclei come together as described in the finite range liquid drop model, with a much reduced fusion barrier. A model for fission would be essentially the same problem, but in reverse. However, in the case of much lower relative kinetic energy, the nuclei when separated look much like when they are far apart, and encounter a strong force repulsive potential barrier that keeps them separated. In this case we might consider them to interact as independent clusters, instead of as a single deformed liquid drop. There are practical issues with such a picture. In order to get the nuclei to nearly touch with vanishing relative kinetic energy in a fusion experiment, the initial relative kinetic energy would need to be large (and precise), in order to have a finite probability of tunneling through the Coulomb barrier and stopping at close range.

Note that the centripetal potential can supply repulsion at short range in a fission type of model, that could result in a well defined potential minimum for a nuclear molecule. The reason we have not focused on such nuclear molecules here is because of the possibility of (fast) radiative decay to lower energy states with lower angular momentum, and also that high angular momentum nuclear molecule states would be difficult to couple to from the (parent) ground state.

3.3. Simple Model for Reasonably Stable Nuclear Molecules

All of this suggests the possibility of developing a simple and crude model to approximate the binding energy of two clusters making up a reasonably stable nuclear molecule, as well as allowing for an estimate of the tunneling rate. It would be possible to use the FRLDM and optimize the surfaces of separated daughter nuclei as a function of the center of mass separation, which would allow us to capture the increased attraction due to the nuclear deformation that occurs in liquid drop models (for separated daughters). However, there are technical issues associated with multiple branches of solutions (which occur even for the separated problem) and the possibility of deformation sufficiently large as to be nonphysical. These headaches provide motivation to work with a simpler model based on spherical daughters, which is free of these headaches.

The model that we have studied estimates the nuclear molecule binding energy simply based on the difference between the Coulomb and YPE energies for the nuclear molecule configuration and for infinite separation. Assuming somewhat arbitrarily that the surface separation is fixed at 0.5 fm, then we can write

$$-B \ = \ E_C(R_{min}) - E_C(\infty) + E_{YPE}(R_{min}) - E_{YPE}(\infty) + E_D(R_{min}) - E_D(\infty) \tag{19}$$

where B is the binding energy of the nuclear molecule treated as two clusters, and where E_C, E_{YPE} and E_D are the Coulomb energy, Yukawa plus exponential energy, and density correction to the Coulomb energy. From this we can find the excitation energy

$$E_{bc} \ = \ M_B c^2 + M_c^2 - M_a c^2 - B \tag{20}$$

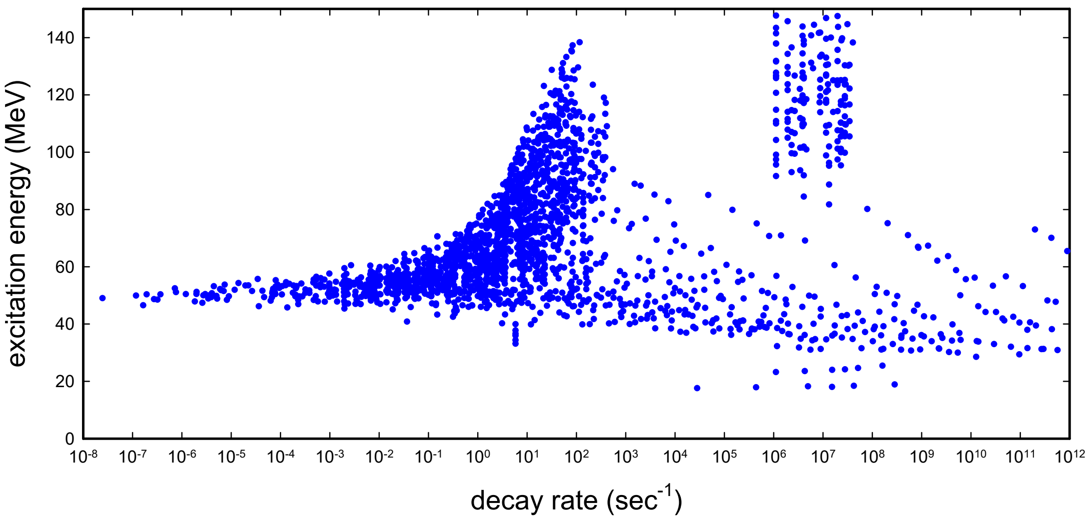

Figure 3. Energy as a function of nuclear molecule decay rate for the stable Pd isotopes.

To estimate the tunneling rate we use

$$\gamma(\text{tunnel}) \;=\; \Gamma_0 e^{-2G} \tag{21}$$

with the Gamow factor estimated using

$$G \;=\; \int_{R_{min}}^{R_{max}} \sqrt{\frac{2\mu(V(r)-E)}{\hbar^2}}dr \tag{22}$$

and

$$\Omega_0 \;=\; \frac{1}{2}\omega_0 \tag{23}$$

where the potential is approximated by

$$V(r) \;\to\; V_0 + \frac{1}{2}\mu\omega_0^2(r-R_{min})^2 \tag{24}$$

with the SHO potential energy taken arbitrarily to be 3 MeV at 1 fm distance from the bottom of the well.

3.4. Results for the Stable Pd Isotopes

We assembled a database for the isotopic mass energies, and used NUDAT3 for the decay rates of the isotopes. We implemented the model described above to determine approximate excitation energies and total (nuclear decay plus tunneling decay) rates for all of the "reasonably stable" nuclear molecules that resulted. Results are shown for the nuclear molecule energy as a function of nuclear molecule decay rate in Figure 3.

We see that according to this model there are hundreds of reasonably stable nuclear molecules, most of which lie above 40 MeV. This is very promising for the nuclear dynamics under consideration in this paper.

Figure 4. Schematic of naive scheme in which the fusion transition down-converts the nuclear energy to vibrational energy.

4. Coherent Energy Exchange

Excess heat in the Fleischmann-Pons experiment is observed without commensurate energetic nuclear products, which is sufficient to rule out incoherent nuclear reactions as a source. For a coherent quantum dynamics scheme to have the maximum overall transition rate, the coherent transitions must be between states that are at the same energy, so that each transition is resonant. Unfortunately, transitions between candidate nuclear states involve keV to MeV energy differences, which cannot be made up with the exchange of a few phonons or plasmons.

Consequently, there needs to be intermediate steps that involve off-resonant states. We have considered these in the context of coherent energy exchange, where interactions between nuclei and vibrations (or plasmons) are modeled in the strong coupling regime. From these models we obtain an effective interaction matrix element which describes indirect coupling between resonant nuclear plus lattice states in which a nuclear transitions occur with the energy difference matched by the change in lattice energy.

In what follows, we consider different possibilities for coherent nuclear dynamics schemes that become possible with different amounts of coherent energy exchange.

4.1. Spin-Boson Approach

Conceptually simple would be a scheme in which the D_2/^{4}He transition was coupled to a highly-excited vibrational mode of the lattice (Figure 4), and one nuclear de-excitation would occur in combination with the (quantum coherent) sequential emission of a large number of quanta satisfying

$$\text{(nuclear energy)} \quad \Delta Mc^2 = \Delta n \hbar\omega_0 \quad \text{(vibrational energy)} \tag{25}$$

Coupling of two-level system energy into oscillator energy through coherent multi-quantum exchange is known for the spin-boson system, so there is precedence for contemplation of such an approach.

Unfortunately, the coupling strength for a Coulomb-hindered fusion transition is very small, and the number of quanta Δn to be transferred is very large, so that the application of the scheme directly to fusion does not work. A modification of the scheme involving a large number of D_2/^{4}He transitions with uniform coupling to a common vibrational mode oscillator can improve the numbers due to the appearance of cooperative Dicke factors, but even with such an enhancement the resulting coherent energy exchange rate is exponentially small.

4.2. Removal of Destructive Interference

Of interest in this discussion is what makes coherent energy exchange slow when Δn is large. One way to think about it is through perturbation theory: in the initial state is a collection of two-level systems in a Dicke state and an excited oscillator with n quanta; and in the final state is essentially the same collection of two-level systems also in a Dicke state, but with one fewer excited states, and where the same excited oscillator now has $n + \Delta n$ oscillator quanta. It is possible to enumerate all of the different pathways through off-resonant states that couple these initial and final states, as well as to sum the contributions from all the different pathways. When this exercise is completed, what is found is that roughly half of the pathways contribute to the sum with a plus sign, and roughly half contribute with a minus sign, so that the total contribution is vanishingly small (when Δn is large).

What prevents coherent energy exchange involving large Δn then is destructive interference. In models where the destructive interference is broken, a dramatic increase in the coherent energy exchange rate is seen [20]–[24].

Two approaches to implement this have been identified. One approach involves decay channels which are significant off of resonance, especially in the case where the energy of an off-resonant state is much less that the available energy (or energy eigenvalue). The energy exchange rate for an idealized model in which all off-resonant states with less energy than the eigenvalue are assumed to decay instantaneously has been quantified [24], [25], [26]. Another approach involves energy level shifts when states are driven off of resonance [27], which can reduce the destructive interference. Unfortunately, there is no such effect at second-order in excitation transfer, in contrast to the discussion given in [27]. The headache in this case was that old-fashioned perturbation theory was used incorrectly in the model discussed, leading to an incorrect conclusion. Had we used a Feynman diagrammatic approach instead, it would have been completely obvious that the nuclei were not off of resonance for second-order excitation transfer, but instead the oscillator. Off-resonant energy shifts of nuclear levels could occur for generalized excitation transfer processes at higher order. Off-resonant energy shifts of nuclear levels would be expected for neutron transfer processes at second order.

It is possible to evaluate conditions under which a great many $D_2/^4He$ transitions transfer 24 MeV to vibrations coherently using this approach (which would also be described by the scheme in Figure 4), with the result that the Dicke-enhanced coupling would only be sufficiently strong with an astronomically large number of transitions. The problem once again is that the Gamow factor associated with tunneling makes the coupling matrix element far too small.

4.3. Excitation Transfer

A much higher overall rate could be obtained if the excitation of the $D_2/^4He$ transition where transferred to produce excitation in other nuclei [27], for example through an excitation process of the form

$$D_2 + Pd \quad \longleftrightarrow \quad ^4He + Pd^*$$

This presumes that there is a reasonably stable highly-excited Pd^* state with an excitation energy matched to the mass difference of the fusion transition. In such a scheme the excitation from a very large number of $D_2/^4He$ transitions is transferred to Pd^*/Pd transitions so that the Dicke-enhanced coupling strength is sufficiently large that the large nuclear quantum can be down-converted through coherent energy exchange (a schematic appears in Figure 5).

The models cited can be used to evaluate conditions under which this much improved scheme might work, and once again the number of transitions involved is many orders of magnitude greater than what is present in Fleischmann-Pons experiments. The problem in this case is that the number of quantum Δn is very large (on the order of 10^9 for an optical phonon mode). Even though down-conversion is greatly accelerated through off-resonant loss processes (which would be expected), it is not accelerated enough to make this approach work.

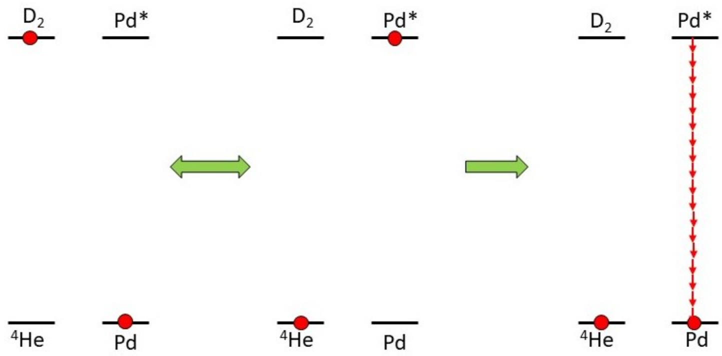

Figure 5. Naive scheme involving excitation transfer followed by down-conversion.

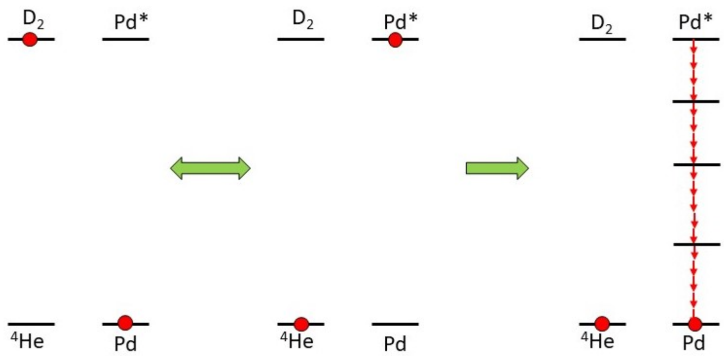

Figure 6. Scheme involving excitation transfer followed by down-conversion with intermediate states.

4.4. Smaller Steps

To address this issue, one approach is to work with smaller steps where the amount of nuclear energy transferred to vibrations is smaller. Conceptually simple (but physically improbable) is a model in which we assume that there are 10 reasonably stable nuclear states equi-spaced between the ground state and the previously assumed excited state at 24 MeV (something like the scheme illustrated in Figure 6). In this model the energy exchange associated with each individual step is $\Delta n/10$, which leads to a reduction of the coupling strength required by about three orders of magnitude.

Once again, it is possible to quantify how many D_2/^{4}He transitions and Pd*/Pd transitions are needed to achieve an overall coherent fusion and down-conversion rate on the order of what is seen in experiments. The result is that the number of transitions is many orders of magnitude greater than is present in the experiments.

The contemplation of this example informs us of the importance of the need for a high density of reasonably stable excited states, which motivates us to ask where the highest density of nuclear molecule states are in Pd. From the results shown in Figure 3 we find that the highest density of nuclear molecule states lies up above about 50 MeV. The average energy difference between the nearest neighbors in a naive picture in which there is only one nuclear molecule per A_b, Z_b value can be as low as about 12 keV. This is encouraging, since the conditions required to transfer 12 keV are much more favorable than 24 MeV or 2.4 MeV.

It is discouraging that the number of transitions needed based on the cited coherent energy exchange models is still orders of magnitude more than experiment even for a down-conversion of only 12 keV.

4.5. Modeling

In preparation for ICCF24 it became clear that nuclear molecule states might offer a real opportunity for there to be reasonably stable excited states that could be used to implement coherent nuclear dynamics driven by coupling with vibrations (or other condensed matter collective degrees of freedom). This focused attention on the coherent energy transfer problem, where it became clear that the energy transfer possible to phonons from the lossy spin-boson model analyzed previously was not going to be sufficient to account for excess heat production in the Fleischmann-Pons experiment. New models that were stronger were needed.

In our ICCF24 presentation preliminary results were presented for models in which external fluctuations were introduced (to help increase the spread of the oscillator distributions in n) and combined with the off-resonant energy shift mechanism. In the calculations done prior to the meeting, this approach looked very attractive, and simulations with relatively small numbers of quanta exchanged looked very promising. Following the conference the scaling of these models was studied with more powerful tools, and it was found that they scaled poorly for large Δn.

We subsequently considered models in which fluctuations in one mode were introduced via coupling through a nonlinearity with another mode. An example of this kind of model is

$$\hat{H} = \hbar\omega_O \hat{a}_O^\dagger \hat{a}_O + \hbar\omega_A \hat{a}_A^\dagger \hat{a}_A + \Delta E \frac{\hat{S}_z}{\hbar} - i\frac{\hbar\Gamma(E)}{2} + V_O \frac{\hat{S}_x}{\hbar}\left(\hat{a}_O^\dagger + \hat{a}_O\right) + V_A \frac{\hat{S}_x}{\hbar}\left(\hat{a}_A^\dagger + \hat{a}_A\right) + K\left(\hat{a}_O^\dagger + \hat{a}_O\right)^2\left(\hat{a}_A^\dagger + \hat{a}_A\right) \tag{26}$$

In this model many two-level systems couple uniformly to acoustic and optical phonon modes that are coupled nonlinearly. Models analyzed based on this approach looked interesting, and appeared to lead to increased coherent energy exchange. After some thought, it was not obvious that there could be a dramatic increase in the coherent energy exchange of optical phonons with dynamics on a sub-picosecond times scale due to a minor interaction with acoustic phonons with dynamics on a microsecond time scale.

Under consideration then are models more closely connected to the originally lossy spin-boson model, in which the nuclei interact linearly with acoustic and optical phonons, as well as with plasmons. The interactions with acoustic phonons appear to be important in developing coherence among a large number of nuclei, while the interactions with optical phonons and plasmons are important for coherent energy exchange. The much larger energy quantum of the plasmons provides for a larger possible total coherent energy exchange.

4.6. Discussion

The conclusion for now is that with optical phonons coherent energy exchange up to on the order of 100 eV should be possible due to coupling with optical phonons, and coupling with plasmons could increase this to on the order of 10 keV. In Figure 7 is shown the density of ground state binary nuclear molecule states with combined nuclear and tunneling decay rates less than 10^{-9} sec^{-1}. The peak density of these states is near one state every 12 keV, which provides for optimism that sequential coherent transitions might be able to convert nuclear energy to plasmon and vibrational energy efficiently in a coherent nuclear dynamics scheme.

However, the situation is much more complicated. The inclusion of spin and angular momentum degrees of freedom for the daughter nuclei, then the density of states would be much larger. Similarly, the inclusion of rotational excitation

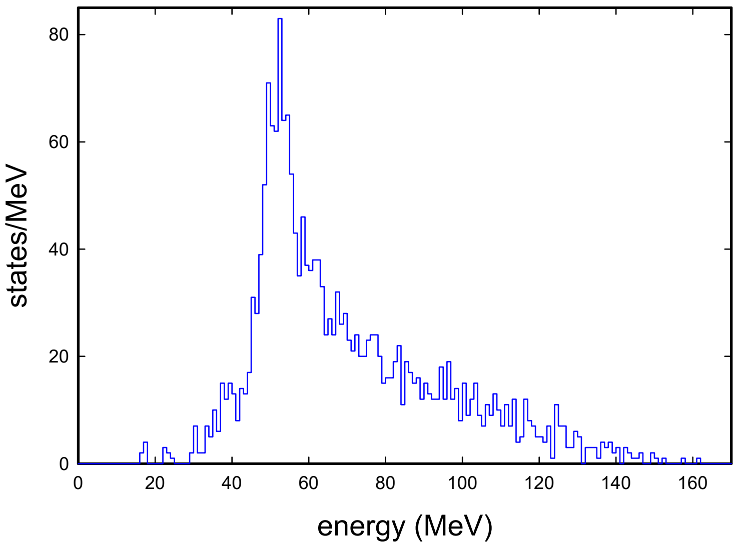

Figure 7. Histogram made from 1 MeV bins from LDM binary nuclear molecule energies from the stable Pd isotopes with decay rates less than 10^9 sec^{-1}.

and vibrational excitation of the nuclear molecule states would also greatly increase the density of states. There are also ternary and quaternary nuclear molecules, which if included would again increase the density of states. But what is important is that there can be low-order coupling from the ground states of the stable Pd isotopes to these nuclear molecule states, so that only a small fraction of these states would be expected to be relevant for the coherent dynamics schemes under consideration.

More complications arise when decay mechanisms are considered. We would expect a modification of the decay rates for the daughters when they are in a nuclear molecule configuration, as the decay energy can be changed. If there are low-order couplings from the ground state directly to these highly-excited nuclear molecule states, then we would expect fast radiative decay rates (as well as internal conversion rates), which suggests that the coupling from the ground state would have to be indirect for things to work.

It is possible that Dicke-enhanced fast excitation transfers between resonant nuclear molecule states could slow down or prevent the (local) decay of these states, by interrupting the accumulation of probability amplitude in the decay channels. In the literature there are many papers on what is called the quantum Zeno effect [28], [29], in which the decay of an excited state is interrupted through measurements. In our case, it would not be measurements that would impact the decay rate, but instead fast transitions to other states. Conceptually this is sufficiently close to the spirit of what is in the literature that it would be appropriate for us to refer to such stabilization as a quantum Zeno effect.

5. A Scenario for Excess Heat and Transmutation

Given the discussion in the sections above, it is clear that there may be a real opportunity working with nuclear molecule states to develop a coherent dynamics scheme that might be relevant to excess heat, transmutation, and other effects seen in LENR experiments. It is also clear that things are not going to be simple.

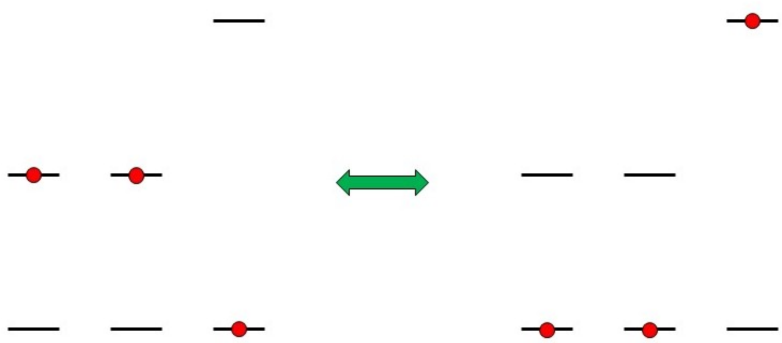

Figure 8. Schematic of a third-order excitation transfer process, where the excitation in two nuclear systems is transferred to a third.

5.1. Initial Excitation Transfer Step

To model excess heat production, the first step has to be the transfer of excitation from the fusion system to another nuclear excited state, since the coupling strength in the case of the fusion system is negligible because of hindrance due to Coulomb repulsion. We would not expect reasonably stable (undeformed) excited states in the stable Pd isotopes near 24 MeV since fast decay by proton, neutron and alpha ejection is possible. The density of nuclear molecule states near this energy is quite low (a few per MeV). A few Ru+^{6}He states are predicted in the general vicinity of D_2/^{4}He transition energy; however, the likelihood of a resonance is very small. An increased probability results if we consider nuclear molecule resonances due to impurity nuclei. Even so, it is very unlikely that a suitable resonant nuclear molecule state exists.

There is the "null" reaction which involves the transfer of excitation from the D_2/^{4}He fusion transition to a ^{4}He/D_2 transition. On the face of it, such a reaction does not seem to be useful. The issue here is that in the present context where many D_2/^{4}He transitions are present, and many ^{4}He nuclei are present to accept the excitation, that a compact D_2^* state is possible in which two deuterons created from the ^{4}He nucleus have trouble tunneling to Angstrom scale separation due to hindrance by the Coulomb barrier. Such a compact state is not expected for the 4-body system in vacuum – it is specific to an excitation transfer system. It may be that such D_2^* compact states are critical to excess heat production in PdD_x, as D_2^*/^{4}He transitions can accept excitation from D_2/^{4}He fusion transitions on resonance.

5.2. Promotion to Higher Energy States

Next, the system needs a way to promote excitation to much higher energy in order to access the high density of states above 40 MeV. Excitation transfer is a second-order process which can move excitation from an excited state at one energy to another at a nearby energy. If the Dicke-enhanced coupling is sufficiently strong, then there is the possibility that a third-order process might occur. Among the different third-order processes possible is one in which two excited nuclear molecules make transitions to the ground state, one a ground state nuclear molecule make a transition to an excited nuclear molecule state at twice the energy (as illustrated in Figure 8). This mechanism would allow promotion of excitation to twice the fusion energy (47.7 MeV) starting from nuclear molecules near the fusion energy. There are many nuclear molecule states nearby this energy. Note that if compact D_2 states are created in the initial transfer step, then low-order coupling would be very strong, favoring higher-order processes.

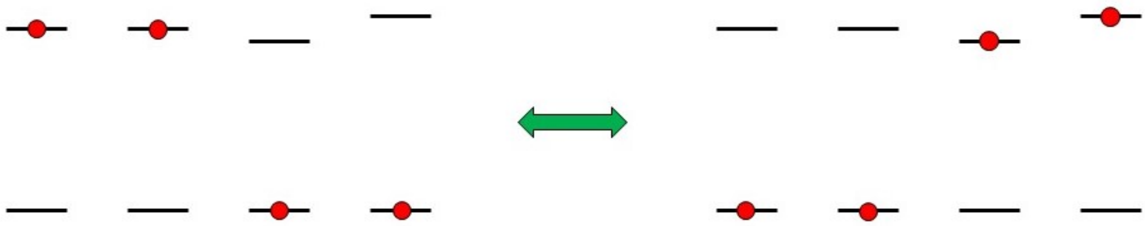

Figure 9. Schematic of a fourth-order excitation transfer process, where the excitation in two nuclear systems is transferred to two other nuclear systems.

5.3. Energy Exchange with Vibrations

With access to states at two times the fusion energy, the system has access to where the density of reasonably stable nuclear molecule states is high. If coherent energy exchange with the lattice per (nonresonant) excitation transfer step can be more than 10 keV, then it is possible that the accessible reasonably stable nuclear molecule density of states is sufficiently high to support excess heat in a scheme only requiring second-order excitation transfer. This would be the simplest possible scenario, and it looks at this point like a viable option.

In the event that coherent energy exchange transfers an energy less than the characteristic energy difference between neighboring states, then we might contemplate generalized excitation transfer processes that occur at higher order. For example, at fourth-order there are processes (illustrated in Figure 9) that can be thought of as transferring excitation between a pair of nuclear molecule states. In this case the pair density of states is much higher (see Figure 10 below), and it becomes much easier for the coherent energy exchange transfers to exceed the energy difference between neighboring states (potentially 10s of eV might be sufficient).

If excess heat is produced via simple second-order excitation transfers, then it may be that excess heat is produced more efficiently (and at a higher rate) if the system enters into a regime in which the fourth-order generalized excitation transfer process becomes dominant.

5.4. Pair Density of States for the Stable Pd Isotopes

The pair density of states can be found from the convolution

$$\rho_2(E) \;=\; (\rho_1 * \rho_1)(E) \;=\; \int_{-\infty}^{\infty} \rho_1(\epsilon)\rho_1(E-\epsilon)d\epsilon \tag{27}$$

Results for the pair density of states with single nuclear molecule decay rate less than 10^9 sec^{-1} is shown in Figure 10. There are additional issues to be considered. Due to the different spin and angular momentum states possible (and relative orientation of oblate and prolate daughters), both the density of states and pair density of states will be significantly larger. Not all of them are expected to be reachable through low-order interactions with phonons and plasmons.

5.5. End-Point of the Dynamics

Suppose now that either second-order or fourth-order (or both) excitation transfer processes are successful in allowing step-by-step transfer of nuclear energy to vibrational and plasmon energy from 3 times the fusion energy down to 2

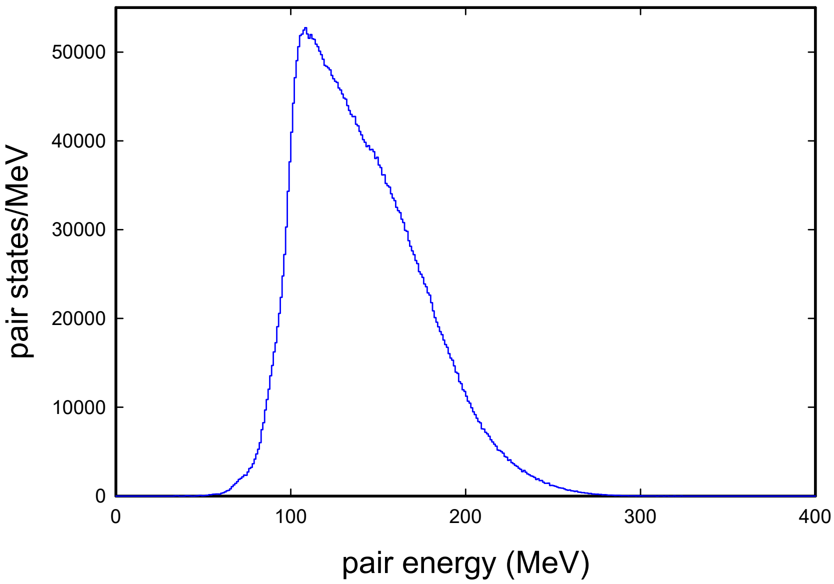

Figure 10. Histogram of the pair density of states for nuclear molecules of the Pd isotopes with decay rates less than 10^9 sec^{-1}.

times the fusion energy. In this case a return to the ground state is possible a third-order processes. The promotion of excited nuclei up to where the high density of states occurs is balanced by downward transitions, as long as there is a constant substantial excited population needed to provide sufficiently large Dicke enhancement factors. This is shown schematically in Figure 11, where for simplicity it is assumed that nearly resonant nuclear molecule states are available among the Pd isotopes for the third-order upward and downward transitions.

Sustained excess he production in this model depends on the excitation of the optical and acoustic phonons, plasmons, as well as maintaining a pool of fusion transitions upon which to draw. If for some reason these falter, and if the system loses the ability to have coherent energy exchange at the level needed for sequential transitions to neighboring nuclear molecule states, then the excess heat cycle would be expected to break. Excited nuclear molecules that are promoted would ultimately be left stranded to decay by tunneling, resulting in a transmutation effect.

6. Coherent Nuclear Dynamics

The coherent nuclear dynamics that result from the ideas outlined above is complicated, and as yet there are no simulation results which might clarify whether the scheme works or not. Nevertheless, it is possible to give a brief outline of the model.

6.1. Coherent Energy Exchange and Degenerate State Transitions

Were we to begin with a basic description of the system starting at the point of single phonon and plasmon exchange, the resulting coherent dynamics calculation would be very complicated and non-intuitive. There would be a messy

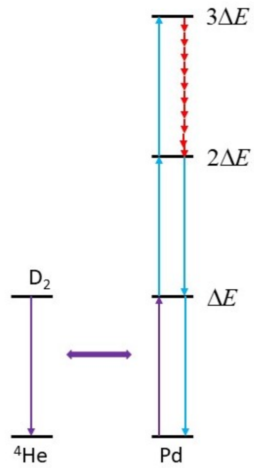

Figure 11. Schematic of excess heat production scheme in Pd. The initial (second-order) excitation transfer from the fusion transition is in purple; the upward and downward transition resulting from third-order interactions are in light blue; and the great many second-order or fourth-order transitions responsible for the primary energy exchange with the lattice are shown in red.

mix of resonant and off-resonant interactions, with off-resonant loss processes critical for the acceleration of excitation transfer processes and coherent energy exchange. Instead of working with such a complicated model, things are simpler if the problem is split into two simpler pieces.

Some years ago we analyzed coherent energy exchange in the case of a lossy spin-boson model, where the loss is asymmetric in the off-resonant energy [24], [25], [26]. What we found can be summarized according to

$$\text{direct}: \quad V_0 \quad \rightarrow \quad V_0 \frac{\Phi}{(\Delta n)^2} \quad : \text{indirect} \tag{28}$$

In essence, the direct interaction strength for a single quantum exchange V_0 leads to an indirect coupling strength between degenerate states that is reduced by a hindrance factor $\Phi/(\Delta n)^2$), where nuclear energy is transferred to the oscillator according to

$$\Delta E \ = \ \Delta n \hbar \omega_0 \tag{29}$$

This observation is key to our thinking. It provides a way to separate the coherent energy exchange calculation from the coherent nuclear dynamics model involving transitions between a sequence of degenerate states.

Based on this observation, we can understand the much more complicated model through two separate simple models. One of these involves the calculation of hindrance factors associated with coherent energy exchange. The other involves modeling sequential coherent transitions between a sequence of resonant states that the system evolves through. In this section our focus is on the coherent nuclear dynamics between the degenerate states.

6.2. Hamiltonian

If we can separate the coherent energy exchange calculation, then we end up with a coherent nuclear dynamics calculation involving (nuclear $\otimes$ phonon $\otimes$ plasmon) states which have the same energy. The indirect coupling matrix elements involved not only describe the coupling required for the nuclear transitions of interest, but also the hindrance that comes from coherent energy exchange that involves a great many individual interactions with the oscillators in which one quantum is exchanged at a time.

In this case, the dynamics discussed in the previous section can be described by a Hamiltonian involving only resonant terms, including transitions due to second-order interactions (for excitation transfer), as well as a subset of the third-order interactions (which promote excitation to get to the high density of states region, and subsequently bring excitation back down), and a subset of the fourth-order interactions (which takes advantage of pairs of transitions which have close initial and final states). Such a model can be expressed as

$$\begin{aligned}\hat{H} = & \sum_j \frac{1}{2}\hbar\Omega_{f,j}\left(\frac{S_+^f}{\hbar}\frac{S_-^j}{\hbar} + \frac{S_-^f}{\hbar}\frac{S_+^j}{\hbar}\right) \\ & + \sum_{j\neq k} \frac{1}{2}\hbar\Omega_{j,k}\left(\frac{S_+^j}{\hbar}\frac{S_-^k}{\hbar} + \frac{S_-^j}{\hbar}\frac{S_+^k}{\hbar}\right) \\ & + \sum_{j,k,l} \frac{1}{2}\hbar\Omega_{j,k,l}\left(\frac{S_+^j}{\hbar}\frac{S_-^k}{\hbar}\frac{S_-^l}{\hbar} + \frac{S_-^j}{\hbar}\frac{S_+^k}{\hbar}\frac{S_+^l}{\hbar}\right) \\ & + \sum_{j,k,l,m} \frac{1}{2}\hbar\Omega_{j,k,l,m}\left(\frac{S_+^j}{\hbar}\frac{S_+^k}{\hbar}\frac{S_-^l}{\hbar}\frac{S_-^m}{\hbar} + \frac{S_-^j}{\hbar}\frac{S_-^k}{\hbar}\frac{S_+^l}{\hbar}\frac{S_+^m}{\hbar}\right)\end{aligned} \tag{30}$$

where the first set of terms account for the transfer of excitation from the fusion system to the compact states D_2^*, and the second set of terms account for excitation transfers between nuclear molecule states. The third and fourth set of terms account for higher-order excitation transfer processes, as discussed above. This Hamiltonian makes use of pseudo-spin operators ($\mathbf{S}^j = \sum_a \mathbf{s}_a^j$) to keep track of level populations, and treats many-level systems as if they acted as simple two-level systems for individual transitions.

6.3. Fusion to Compact State Interaction Strength

The general form of the degenerate Hamiltonian above is determined by the nuclear states involved in the scheme described in the previous section. The rate at which the nuclear coherent dynamics evolves is determined by the interaction strengths, which we consider briefly in this subsection.

The strength of the first excitation transfer step is of the form

$$\hbar\Omega_{f,j} \ = \ 2\frac{(\mathbf{a}\cdot c\mathbf{P})_f(\mathbf{a}\cdot c\mathbf{P})_j}{\Delta E_{f,j}}\left(\sqrt{\frac{V_{nuc}}{V_{mol}}}e^{-G}\right)_f \tag{31}$$

The individual transitions are assumed here to be M2 transitions mediated by the relativistic phonon-nuclear interaction [30], where the $\mathbf{a}$ are internal nuclear transition matrix elements, and where $\mathbf{P}$ is the center of mass momentum of the 4-body system for the fusion system (f) and for the compact state system (j). Note that there are quite a few molecular D_2 states possible (^{1,5}S, ^{3}P, $\cdots$), and the M2 interaction here focuses on coupling to ^{3}P molecular D_2 states. In this expression the Gamow and volume factors have been extracted from the nuclear M2 $\mathbf{a}$-matrix element to emphasize that this transition is hindered due to Coulomb repulsion. Note that the coherent dynamics rate can be on the order of the magnitude of the indirect coupling matrix element divided by $\hbar$, which means that it can be linear in e^{-G}, where incoherent fusion reactions scale as e^{-2G}. This makes explicit that the coherent dynamics can potentially be orders of magnitude faster than the rate of incoherent fusion decays. Note that indirect coupling associated with excitation transfer would have this form in the limit that off-resonant loss removes destructive interference completely, which requires that $\hbar\Gamma$ is much larger than the transition energy ΔE.

6.4. Interaction Strength for Nuclear Molecule Transitions

The simplest possible model for interactions between nuclear molecule transitions is

$$\hbar\Omega_{j,k} \ = \ 2\frac{(\mathbf{d}\cdot\mathbf{E})_j(\mathbf{d}\cdot\mathbf{E})_k}{\Delta E_{j,k}}\frac{\Phi_{j,k}}{(\Delta n)^2_{j,k}} \tag{32}$$

where we assume that transitions between the stable Pd isotope ground states and nuclear molecule states are mediated by electric dipole transitions. Also possible are magnetic dipole transitions mediated by oscillating magnetic fields associated with spin-wave modes, and M2 transitions mediated by the relativistic phonon-nuclear interaction. Once again, we assume that off-resonant loss eliminates destructive interference, leading to the form of the interaction. We expect a hindrance factor $\Phi/(\Delta n)^2$ analogous to what we found previously [24]-[26], except that a new model will be needed to evaluate it since two-quantum exchange is possible for individual excitation transfer steps (where the earlier models were analyzed for one-quantum exchange). Also, it is clear now that the calculations are going to need to extend to a range of stronger coupling than what was considered previously.

There are issues involved in connection with the evaluation of the dipole moment for these transitions. When first proposed we anticipated small dipole moments, perhaps in the range of $10^{-8} - 10^{-5}$ e-fm, primarily since if the dipole moments were larger the radiative decay rates would seem to be too fast. However, more recently we have understood that to connect with experiment the dipole moments will need to be much larger. Such large dipole moments for direct transitions seem to be problematic due to the fast associated radiative decay. It is likely that the coupling would need to be indirect, so that radiative transitions directly back down to the Pd ground states are forbidden. The thought is to consider models written in terms of low-order coupling for now, and move to indirect transitions when the models are better understood.

The specification of coupling strengths for the higher-order transitions included in the Hamiltonian would work similarly.

6.5. Ehrenfest Theorem Dynamics

The dynamics of the expectation values can be determined using Ehrenfest's theorem, which might be written for a general operator $\hat{Q}$ as [31]

$$\frac{d}{dt}\langle\hat{Q}\rangle \ = \ \left\langle\frac{\partial\hat{Q}}{\partial t}\right\rangle + \frac{1}{i\hbar}\left\langle[\hat{Q},\hat{H}]\right\rangle \tag{33}$$

This approach is often used to develop equivalent classical equations of motion for a quantum mechanical model.

For the model described above, we can write for the fusion transitions

$$\begin{aligned}
\frac{d}{dt}S_x^f &= \sum_k \Omega_{k,f}\frac{S_y^k}{\hbar}S_z^f \\
\frac{d}{dt}S_y^f &= -\sum_k \Omega_{k,f}\frac{S_x^k}{\hbar}S_z^f \\
\frac{d}{dt}S_z^j &= \sum_k \Omega_{k,f}\left(\frac{S_x^k}{\hbar}S_y^f - \frac{S_y^k}{\hbar}S_x^f\right)
\end{aligned} \tag{34}$$

For the excited nuclear molecule transitions we have

$$
\begin{aligned}
\frac{d}{dt}S_x^n = &\sum_f \Omega_{f,n}\frac{S_y^f}{\hbar}S_z^n + \sum_k \Omega_{k,n}\frac{S_y^k}{\hbar}S_z^n \\
&+ \sum_{k,l}\Omega_{n,k,l}\left(\frac{S_x^k}{\hbar}\frac{S_y^l}{\hbar} + \frac{S_y^k}{\hbar}\frac{S_x^l}{\hbar}\right)S_z^n + \sum_{j,l}\Omega_{j,n,l}\left(\frac{S_y^j}{\hbar}\frac{S_x^l}{\hbar} - \frac{S_x^j}{\hbar}\frac{S_y^l}{\hbar}\right)S_z^n \\
&+ \sum_{k,l,m}\Omega_{n,k,l,m}\left(\frac{S_x^k}{\hbar}\left(\frac{S_y^l}{\hbar}\frac{S_x^m}{\hbar} + \frac{S_x^l}{\hbar}\frac{S_y^m}{\hbar}\right) + \frac{S_y^k}{\hbar}\left(\frac{S_y^l}{\hbar}\frac{S_y^m}{\hbar} - \frac{S_x^l}{\hbar}\frac{S_x^m}{\hbar}\right)\right)S_z^n
\end{aligned}
\tag{35}
$$

$$
\begin{aligned}
\frac{d}{dt}S_y^n = &-\sum_f \Omega_{f,n}\frac{S_x^f}{\hbar}S_z^n - \sum_k \Omega_{k,n}\frac{S_x^k}{\hbar}S_z^n \\
&+ \sum_{k,l}\Omega_{n,k,l}\left(\frac{S_y^k}{\hbar}\frac{S_y^l}{\hbar} - \frac{S_x^k}{\hbar}\frac{S_x^l}{\hbar}\right)S_z^n - \sum_{j,l}\Omega_{j,n,l}\left(\frac{S_x^j}{\hbar}\frac{S_x^l}{\hbar} + \frac{S_y^j}{\hbar}\frac{S_y^l}{\hbar}\right)S_z^n \\
&- \sum_{k,l,m}\Omega_{n,k,l,m}\left(\frac{S_x^k}{\hbar}\left(\frac{S_x^l}{\hbar}\frac{S_x^m}{\hbar} - \frac{S_y^l}{\hbar}\frac{S_y^m}{\hbar}\right) + \frac{S_y^k}{\hbar}\left(\frac{S_y^l}{\hbar}\frac{S_x^m}{\hbar} + \frac{S_x^l}{\hbar}\frac{S_y^m}{\hbar}\right)\right)S_z^n
\end{aligned}
\tag{36}
$$

$$
\begin{aligned}
\frac{d}{dt}S_z^n = &\sum_f \Omega_{f,n}\left(\frac{S_x^f}{\hbar}S_y^n - \frac{S_y^f}{\hbar}S_x^n\right) + \sum_k \Omega_{k,n}\left(\frac{S_x^k}{\hbar}S_y^n - \frac{S_y^k}{\hbar}S_x^n\right) \\
&- \sum_{k,l}\Omega_{n,k,l}\left(\frac{S_y^k}{\hbar}\frac{S_x^l}{\hbar} + \frac{S_x^k}{\hbar}\frac{S_y^l}{\hbar}\right)S_x^n + \sum_{k,l}\Omega_{n,k,l}\left(\frac{S_x^k}{\hbar}\frac{S_x^l}{\hbar} - \frac{S_y^k}{\hbar}\frac{S_y^l}{\hbar}\right)S_y^n \\
&- \sum_{j,l}\Omega_{j,n,l}\left(\frac{S_y^j}{\hbar}\frac{S_x^l}{\hbar} + \frac{S_x^j}{\hbar}\frac{S_y^l}{\hbar}\right)S_x^n + \sum_{j,l}\Omega_{j,n,l}\left(\frac{S_x^j}{\hbar}\frac{S_x^l}{\hbar} - \frac{S_y^j}{\hbar}\frac{S_y^l}{\hbar}\right)S_y^n \\
&+ \sum_{k,l,m}\Omega_{n,k,l,m}\left(-\frac{S_x^k}{\hbar}\left(\frac{S_x^l}{\hbar}\frac{S_y^m}{\hbar} + \frac{S_y^l}{\hbar}\frac{S_x^m}{\hbar}\right) + \frac{S_y^k}{\hbar}\left(\frac{S_x^l}{\hbar}\frac{S_x^m}{\hbar} - \frac{S_y^l}{\hbar}\frac{S_y^m}{\hbar}\right)\right)S_x^n \\
&+ \sum_{k,l,m}\Omega_{n,k,l,m}\left(\frac{S_x^k}{\hbar}\left(\frac{S_x^l}{\hbar}\frac{S_x^m}{\hbar} - \frac{S_y^l}{\hbar}\frac{S_y^m}{\hbar}\right) + \frac{S_y^k}{\hbar}\left(\frac{S_y^l}{\hbar}\frac{S_x^m}{\hbar} + \frac{S_x^l}{\hbar}\frac{S_y^m}{\hbar}\right)\right)S_y^n
\end{aligned}
\tag{37}
$$

The dynamical equations can be augmented with loss terms to account for tunnel decay of the nuclear molecules for transmutation and for low-level nuclear emissions. This involves the replacement of the time derivatives according to [31]

$$
\frac{d}{dt}\mathbf{S}^n \;\rightarrow\; \frac{d}{dt}\mathbf{S}^n + \frac{\mathbf{S}^n}{\tau_n}
\tag{38}
$$

The pseudo-spin dynamics can be augmented with dynamical equations for the optical and acoustic phonon modes, to provide a more complete overall system description. Most of the energy transferred in this model would go into the optical phonon mode simply because the energy quantum is larger; nevertheless some goes into the acoustic mode, and how much can be determined from a coherent energy transfer model.

6.6. Discussion

To see whether the model under discussion is successful in describing excess heat, transmutation, and also low-level nuclear emissions we are going to need to solve the dynamical equations. A challenge is that on the general order of a thousand transitions would ideally need to be modeled for excess heat, which suggests that it would be appropriate to develop various reduces and simplified versions of the model that are easier to understand and analyze. A headache is that we will likely never have accurate values for the excited state nuclear molecule energies or for the transition matrix elements. So most likely we face using the models to understand what range of transition matrix element magnitudes are consistent with experiment through this kind of model.

7. Conclusions

Early models for deuteron-deuteron fusion based on the Golden Rule are conceptually simple, and reasonably straightforward to evaluate. For such a calculation one requires a specification of the initial state, the final state, and the model nuclear potential [32]. With the evaluation of the transition matrix element, and combining the square with the density of states and a prefactor, one arrives at the fusion cross section which with only modest overall effort connects reasonably well with experiment.

Contrast this with all of the various calculations that appear to be needed to evaluate the model for coherent deuteron-deuteron fusion as outlined in this paper. The conclusion is that excess heat in the Fleischmann-Pons experiment is much more complicated. It is not surprising that an appropriate theory did not emerge during the early days of the field, as the focus was on conceptually simple explanations and approaches. Nevertheless, if excess heat works as outline in this paper, then it is understandable and we can work with it.

The number of issues raised in this paper is very large, and here only a few will be considered.

It is conceptually simplest to imagine that a nuclear molecule from a Pd isotope will have a reasonably close resonance with the $D_2/^4He$ fusion transition. However, there is no guarantee that the resonance will be good enough. It may be that there will be a close resonance for excitation to a reasonably stable nuclear molecule is some isotope, and perhaps this isotope is an impurity in the cathodes used. A precise resonance is guaranteed for $^4He/D_2^*$ excitation, which involves a compact D_2^* state.

The density of states is much higher in the vicinity of $2\Delta E$, so as long as sufficient coherent energy exchange is possible, these transitions should work OK.

For third and fourth-order excitation processes to become important and to play a significant role in the coherent nuclear dynamics, the coupling must be strong. In the model outlined above, this can occur if large Dicke enhancement factors occur (which means that the quantity $|\hat{\mathbf{i}}_z \times \mathbf{S}|$ associated with the relevant pseudostate $\mathbf{S}$-vectors must be large). This is consistent with a larger number of fusion transitions and relevant nuclear molecule transitions being coupled to a common highly-excited acoustic phonon mode, which could be if a larger sample is involved, and if the amplitudes of the acoustic and optical phonon mode amplitudes are large (same for the plasmon mode amplitude).

There does not seem to be anything in principle to prevent an LENR system from reaching a regime in which the coupling is sufficiently strong that fourth-order (or even higher-order) interactions become important.

We previously speculated that low-level energetic alpha decay might be due to nuclear molecules in which one of the daughters is an alpha particle. It is clear from the simple nuclear molecule model above that such states would be expected to decay rapidly, which would be consistent with a low-level emission process. The same kind of mechanism would apply to low-level emission of other light particles.

If the coupling between the Pd ground state nuclei and nuclear molecules is of low order, then we would expect low-level gamma emission above 40 MeV. Such gammas would be detectable, and if seen would provide strong confirmation of the models under discussion. More likely, the coupling to these levels would be indirectly, and gamma emission suppressed.

In the coherent reaction scheme proposed here there is a clear connection between excess heat production and transmutation. The two go hand in hand, and transmutation at low levels would be expected during excess heat production. Massive transmutation would mean that the system is close to producing excess heat, but frustrated by an increasing spacing between pairs as transitions occur further and further from the nuclear molecule band head. The model suggests that some excess heat production occurs in connection with transmutation, and that what transmutation daughters are produced depends on how much coherent energy transfer occurs. This implies that it may be possible to eventually provides some control over which transmutation daughters are produced in an experiment.

For coherent energy exchange the discussion focused on the special case involving a uniform acoustic phonon mode and a uniform optical phonon mode with nonlinear coupling, but it is clear that this is not the only possibility. It would be expected that a strongly excited uniform acoustic mode would be important (since it is easy to excite, and can couple the largest number of nuclei); however, it is probable that generalizations of the model will work for multiple optical phonon modes with less uniform interactions, as well as indirect coupling with plasmon modes (as well as other condensed matter collective modes). Intuitively, the nuclear transitions need to dump energy for the process to proceed, and the larger the quantum of the collective mode, the fewer quanta need to be exchanged, and potentially the more efficient the system can work (within the constraints mentioned previously, such as the requirement for strong Dicke-enhanced coupling).

Note that while the discussion has focused on nuclear molecule states as candidate excited states that are reasonably stable, the same ideas and approach is relevant to coupling in the case of metastable excited nuclear states, except that the coupling would involve higher multipolarity than electric dipole coupling.

Finally, it seems clear that we are going to need to develop reduced versions of the model that are more easily analyzed and worked with.

Note added in proof: It was also understood after the paper was accepted that the compact D_2^* excited states are all unstable to fast 3+1 decay, so they cannot be doorway states for promotion to nuclear molecule states at $2\Delta E$. I was also understood after the paper was accepted that the $\mathbf{a} \cdot c\mathbf{P}$ interaction leads to matrix elements orders of magnitude larger than for the $-\mathbf{d} \cdot \mathbf{E}$ interaction, so that it is likely that all important transitions in the model will be mediated by the $\mathbf{a} \cdot c\mathbf{P}$ interaction.

References

[1] P. L. Hagelstein and I. U. Chaudary, "Anomalies in fracture experiments, and energy exchange between vibrations and nuclei," *Meccanica* **50** (2015) 1189–1203.

[2] D. A. Bromley, J. A. Kuehner and E. Almqvist, "Resonant elastic scattering of C^{12} by carbon," *Phys. Rev. Lett.* **4** (1960) 365.

[3] E. Almqvist, D. A. Bromley and J. A. Kuehner, "Resonances in C^{12} on carbon reactions," *Phys. Rev. Lett.* **4** (1960) 515.

[4] E. Vogt and H. McManus, " Molecular states formed by two carbon nuclei," *Phys. Rev. Lett.* **4** 518.

[5] N. Bohr and J. A. Wheeler, "The mechanism of nuclear fission," *Phys. Rev.* **56** (1939) 426.

[6] L. G. Moretto, P. T. Lake, L. Phair and J. B. Elliott, "Reexamination and extension of the liquid drop model: Correlation between liquid drop parameters and curvature term," *Physical Review C* **86** (2012) 021303.

[7] Y. Cao, D. Lu, Y. Qian and Z. Ren, "Uncertainty analysis for the nuclear liquid drop model and implications for the symmetry energy coefficients," *Physical Review C* **105** (2022) 034304.

[8] H. J. Krappe, J. R. Nix and A. J. Sierk, "Unified nuclear potential for heavy-ion elastic scattering, fusion, fission, and ground-state masses and deformations," *Phys. Rev. C* **20** (1979) 992.

[9] A. J. Sierk, "Macroscopic model of rotating nuclei," *Phys. Rev. C* **33** (1986) 2039.

[10] P. Möller, A. J. Sierk, T. Ichikawa and H. Sagawa, "Nuclear ground-state masses and deformations: FRDM," *Atomic Data and Nuclear Data Tables* **109** (2012) 1–204.

[11] J. R. Nix and A. J. Sierk, "Potential-energy surfaces for heavy-ion collisions," *Physica Scripta* **10** (1974) 94.

[12] K. T. Davies and J. R. Nix, “Calculation of moments, potentials, and energies for an arbitrarily shaped diffuse-surface nuclear density distribution,” *Physical Review C* **14** (1976) 1977.

[13] R. Bengtsson, P. Möller, J. R. Nix and J. Y. Zhang, “Nuclear shapes and shape transitions,” *Physica Scripta* **29** (1984) 402.

[14] J.R. Nix, “Further studies in the liquid-drop theory on nuclear fission,” *Nuclear Physics A* **130** (1969) 241.

[15] L. Satpathy and P. Sarangi, “Resonances of the bonding potential of ^{12}C+^{12}C system,” *Journal of Physics G: Nuclear and Particle Physics* **16** (1990) 469.

[16] A. Diaz-Torres and M. Wiescher, “Characterizing the astrophysical S factor for ^{12}C+^{12}C fusion with wave-packet dynamics,” *Physical Review C* **97** (2018)055802.

[17] K. Godbey, C. Simenel and A. S. Umar, “Absence of hindrance in a microscopic ^{12}C+^{12}C fusion study,” *Physical Review C* **100** (2019) 024619.

[18] A. Diaz-Torres, L. R. Gasques and M .Wiescher, “Effects of nuclear molecular configurations on the astrophysical S-factor for ^{16}O+^{16}O,” *Physics Letters B* **652** (2007) 255.

[19] C. Simenel, R. E. C. E. P. Keser, A. S. Umar and V. E. Oberacker, “Microscopic study of ^{16}O+^{16}O fusion,” *Physical Review C* **88** (2013) 024617.

[20] P. L. Hagelstein and I. U. Chaudhary, “Energy exchange in the lossy spin-boson model,” *J. Condensed Matter Nucl. Sci.* **5** (2011) 52–71.

[21] P. L. Hagelstein and I. U. Chaudhary, “Dynamics in the case of coupled degenerate states,” *J. Condensed Matter Nucl. Sci.* **5** (2011) 72–86.

[22] P. L. Hagelstein and I. U. Chaudhary, “Second-order formulation and scaling in the lossy spin-boson model,” *J. Condensed Matter Nucl. Sci.* **5** (2011) 87–101.

[23] P. L. Hagelstein and I. U. Chaudhary, “Local approximation for the lossy spin-boson model,” *J. Condensed Matter Nucl. Sci.* **5** (2011) 102–115.

[24] P. L. Hagelstein and I. U. Chaudhary, “Coherent energy exchange in the strong coupling limit of the lossy spin-boson model,” *J. Condensed Matter Nucl. Sci.* **5** (2011) 116–139.

[25] P. L. Hagelstein and I. U. Chaudhary, “Generalization of the lossy spinboson model to donor and receiver systems,” *J. Condensed Matter Nucl. Sci.* **5** (2011) 140–154.

[26] P. L. Hagelstein and I. U. Chaudhary, “Pulse and amplitude approximation for the lossy spinboson model,” *J. Condensed Matter Nucl. Sci.* **9** (2012) 30–49.

[27] P. L. Hagelstein “Phonon-mediated nuclear excitation transfer,” *J. Condensed Matter Nucl. Sci.* (2018) **27** 97.

[28] C. B. Chiu, E. C. G. Sudarshan and B. Misra, “Time evolution of unstable quantum states and a resolution of Zeno’s paradox,” *Physical Review D* **16** (1977) 520.

[29] F. Schäfer, I. Herrera, S. Cherukattil, C. Lovecchio, F. S. Cataliotti, F. Caruso and A. Smerzi, “Experimental realization of quantum zeno dynamics,” *Nature communications* **5** (2014) 3194.

[30] P. L. Hagelstein, “Lowest-order relativistic interaction between lattice vibrations and internal degrees of freedom of a nucleus,” *Journal of Physics B: Atomic, Molecular and Optical Physics* **56** (2023) 195002.

[31] P. L. Hagelstein, S. D. Senturia and T. P. Orlando, *Introductory applied quantum and statistical mechanics*, John Wiley & Sons (2004).

[32] D. U. Yu, “On the question of charge symmetry in D-D reactions,” *Progress of Theoretical Physics* **36** (1966) 734–744.